

**Tilt grain boundaries in a diblock copolymer ordered nanocomposite lamellar phase**

Russell B. Thompson

Citation: *The Journal of Chemical Physics* **133**, 144902 (2010); doi: 10.1063/1.3498784

View online: <http://dx.doi.org/10.1063/1.3498784>

View Table of Contents: <http://scitation.aip.org/content/aip/journal/jcp/133/14?ver=pdfcov>

Published by the [AIP Publishing](#)

---

**Articles you may be interested in**

[Assembly of diblock copolymer functionalized spherical nanoparticles as a function of copolymer composition](#)  
J. Chem. Phys. **140**, 144905 (2014); 10.1063/1.4870592

[Ordered structures of diblock nanorods induced by diblock copolymers](#)  
J. Chem. Phys. **139**, 104901 (2013); 10.1063/1.4819775

[Phase behaviors of diblock copolymer-nanoparticle films under nanopore confinement](#)  
J. Chem. Phys. **130**, 094903 (2009); 10.1063/1.3055601

[Coarse-grained molecular dynamics simulation on the placement of nanoparticles within symmetric diblock copolymers under shear flow](#)  
J. Chem. Phys. **128**, 164909 (2008); 10.1063/1.2911690

[Surface induced ordering in thin film diblock copolymers: Tilted lamellar phases](#)  
J. Chem. Phys. **115**, 1970 (2001); 10.1063/1.1379759

---



**NEW Special Topic Sections**

**NOW ONLINE**  
Lithium Niobate Properties and Applications:  
Reviews of Emerging Trends

**AIP** | Applied Physics  
Reviews

# Tilt grain boundaries in a diblock copolymer ordered nanocomposite lamellar phase

Russell B. Thompson<sup>a)</sup>

Department of Physics and Astronomy, University of Waterloo, 200 University Avenue West, Waterloo, Ontario N2L 3G1, Canada

(Received 7 September 2010; accepted 16 September 2010; published online 8 October 2010)

A hybrid self-consistent field theory/density functional theory method is applied to predict tilt (kink) grain boundary structures between lamellar domains of a symmetric diblock copolymer with added spherical nanoparticles. Structures consistent with experimental observations are found and theoretical evidence is provided in support of a hypothesis regarding the positioning of nanoparticles. Some particle distributions are predicted for situations not yet examined by experiment. © 2010 American Institute of Physics. [doi:10.1063/1.3498784]

## I. INTRODUCTION

Block copolymer nanocomposites, consisting of a self-assembling block copolymer mixed with nonpolymeric particles of nanometer dimensions, represent a nascent approach to nanotechnology.<sup>1</sup> In pure block copolymer systems, material properties and technological applications can be limited by imperfections in the system.<sup>2,3</sup> On the other hand, if these imperfections can be understood and controlled, they could potentially be engineered and used directly for applications.<sup>4</sup> In block copolymers, grain boundaries have been studied both experimentally and theoretically (see, for example, Refs. 5–10). An experimental study by Listak and Bockstaller<sup>11</sup> represents the first attempt to understand grain boundary formation in block copolymer nanocomposites. They combined symmetric diblock copolymer of poly(styrene-*b*-ethylene propylene) with poly(styrene)-coated gold nanocrystals with the result that the particles sequestered preferentially in one of the domains of the diblock copolymer. This groundbreaking study revealed that the presence of nanoparticles affects the frequency of occurrence of certain types of grain boundaries, revealing how the particles affect the block copolymer. It also showed how the particles could be organized in ways that were different from a perfect bulk periodic phase, revealing how the diblock affects the particles. Thus they found different types of control in this system including not just block copolymer self-assembly and colloidal organization, but also grain boundary directed organization. The system is therefore a fertile one for engineering nanoscale structures.

The purpose of the present article is to apply a theoretical methodology to the diblock copolymer/nanoparticle system, in particular to study the effects of nanoparticles on tilt (also called kink) grain boundaries. Specifically, the applicability of a self-consistent field theory/density functional theory (SCFT/DFT) hybrid model is tested for the diblock/nanoparticle system. Since the hybrid SCFT/DFT approach was introduced<sup>12,13</sup> it has been remarkably successful, in a qualitative sense, for a number of different situations

(Refs. 14–20 and references therein) in predicting experimental results (Refs. 1–3, 21, and 22 and references therein) despite having some known limitations.<sup>23</sup> Here, it is found that the trends predicted by the SCFT/DFT theory are consistent with the experimental results of Listak and Bockstaller and that the theory provides evidence in support of their hypothesis regarding the mechanism of particle distribution in nanocomposite tilt grain boundaries. As the theory has been presented in detail elsewhere, only a summary theoretical section with references is provided. This is followed by the results and discussion section and finally by a summary of conclusions and the future outlook.

## II. THEORY

The system to be examined is that of a monodisperse diblock copolymer combined with monodisperse, spherical particles. The SCFT/DFT formalism for this system can be summarized by the free energy functional

$$\begin{aligned} \frac{NF}{\rho_0 k_B T V} = & -\frac{\phi_p}{\alpha} \ln \left( \frac{Q_p \alpha}{V \phi_p} \right) - (1 - \phi_p) \ln \left[ \frac{Q_d}{V(1 - \phi_p)} \right] \\ & + \frac{1}{V} \int d\mathbf{r} [\chi_{AB} N \varphi_A(\mathbf{r}) \varphi_B(\mathbf{r}) \\ & + \chi_{AP} N \varphi_A(\mathbf{r}) \varphi_P(\mathbf{r}) + \chi_{BP} N \varphi_B(\mathbf{r}) \varphi_P(\mathbf{r}) \\ & - w_A(\mathbf{r}) \varphi_A(\mathbf{r}) - w_B(\mathbf{r}) \varphi_B(\mathbf{r}) - w_P(\mathbf{r}) \varphi_P(\mathbf{r}) \\ & + \rho_P(\mathbf{r}) \Psi_{hs}(\bar{\varphi}_P(\mathbf{r}))]. \end{aligned} \quad (1)$$

The left hand side of Eq. (1) is a free energy density (free energy  $F$  divided by system volume  $V$ ) made dimensionless by dividing the thermal energy  $k_B T$  and multiplying the volume of one diblock copolymer  $N/\rho_0$ .  $N$  is the degree of polymerization based on a segment volume  $\rho_0^{-1}$ . On the right hand side,  $\phi_p$  is the overall volume fraction of nanoparticles in the system. The system is modeled as incompressible so that the volume fraction of diblocks must be  $(1 - \phi_p)$ . The ratio of the volumes of one particle to one diblock copolymer is given by  $\alpha$ .  $Q_p$  and  $Q_d$  are the single molecule partition functions for particles and diblocks, respectively. Flory–

<sup>a)</sup>Electronic mail: thompson@uwaterloo.ca.

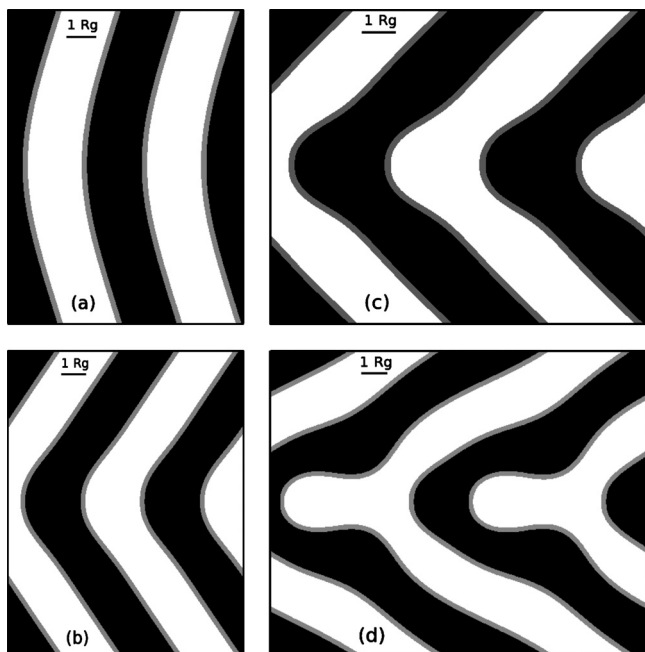


FIG. 1. Tilt grain boundary profiles for a neat, symmetric, diblock copolymer. (a) Low angle chevron boundary. (b) Higher angle chevron boundary. (c) Intermediate boundary. (d) Omega boundary. The gray regions are the  $A/B$  interfacial regions of  $A$  from volume fractions of 0.35–0.67.

Huggins parameters are defined to describe the interactions between different chemical species. These are  $\chi_{AB}$ ,  $\chi_{AP}$ , and  $\chi_{BP}$  between  $A$ -blocks ( $A$ ),  $B$ -blocks ( $B$ ), and particles ( $P$ ). Since they always appear in products with  $N$ , it will be to these products that values are assigned. The local volume fractions  $\varphi_{A,B}$  or  $\varphi_P(\mathbf{r})$  give the morphologies that will be plotted in Sec. III. To find these local volume fractions, the fields  $w_{A,B}$  or  $w_P(\mathbf{r})$  are also needed.  $\rho_p(\mathbf{r})$  is the distribution of particle centers of mass and  $\bar{\varphi}_p(\mathbf{r})$  is a smoothed particle volume fraction defined in a DFT of Tarazona.<sup>24</sup> This DFT uses the Carnahan–Starling equation of state<sup>25</sup> which gives rise to the function  $\Psi_{hs}$  defined, for example, in Refs. 12 and 13.

The relationships between these functions are not provided here, nor are the SCFT equations that can be derived from the free energy functional (1). The reader is rather referred to Refs. 12 and 13. The SCFT equations do require the diblock symmetry  $f$  and the radius of the particles  $R$ . This radius allows us to write the particle to polymer volume ratio  $\alpha$  in terms of

$$\alpha = \frac{4\pi}{3} \frac{1}{6\sqrt{6}} \left(\frac{R}{R_g}\right)^3 \bar{N}^{1/2}, \quad (2)$$

where  $R_g$  is the unperturbed radius of gyration of a diblock copolymer which is taken as the length scale for all distances. From Eq. (2) it is seen that given the particle radius, one can talk in terms of an invariant polymerization index  $\bar{N}$  (Ref. 26) rather than the volume ratio  $\alpha$ .

### III. RESULTS AND DISCUSSION

Figure 1 shows contour plots of some examples of a neat diblock copolymer forming a tilt grain boundary. The panels, from (a) to (d), show an increasing angle between two lamel-

lar grains. The expected range of different types of tilt grain boundaries is seen in this figure including chevron boundaries in panels (a) and (b) through an intermediate boundary in (c) where a protrusion is developing, to an omega boundary (d) where the symmetry between the  $A$  and  $B$  blocks is broken in order to relieve packing frustration.<sup>6,27</sup> These forms of tilt grain boundaries have been previously observed both theoretically<sup>6</sup> and experimentally.<sup>5</sup> While SCFT correctly predicts the (asymmetric) omega phase, it should be noted that other theoretical approaches are unable to produce this experimentally observed feature.<sup>7,8</sup> All calculations in Fig. 1 and in figures that follow were done in real space on a grid of 6400 points converged to a deviation of  $10^{-6}$  in the  $w(\mathbf{r})$  fields according to the definition given in Ref. 28. Anderson mixing<sup>28</sup> was used to speed convergence where appropriate. The diffusion equation was solved using a Crank–Nicolson algorithm with 20 polymer contour steps and with a mixture of periodic and reflecting boundary conditions. It is this mixture of boundary conditions that allows the metastable grain boundary phase to be observed in this real-space implementation of SCFT.<sup>29</sup>

It is to the common forms of tilt grain boundaries shown in Fig. 1 that a representation of particles can be added to test the reliability of the SCFT/DFT formalism. Figure 2 shows contour plot predictions for the same types of grain boundaries as Fig. 1 but with monodisperse nanoparticles of radii  $R=0.5R_g$  added to form a diblock copolymer nanocomposite. An invariant polymerization index of  $\bar{N}=1000$  is taken which produces, from formula (2), an  $\alpha$  value somewhat larger than 1. The particles are assumed to be ideally wet by the  $A$  block, so values of  $\chi_{AB}N=\chi_{BP}N=25$  and  $\chi_{AP}N=0$  are selected. The diblocks are symmetric with  $f=0.5$  and therefore, to remain in the lamellar phase, a low loading of particles of 5% by volume, that is,  $\phi_p=0.05$ , is chosen.

Figure 2(a) shows that the particles, as expected, localize within the  $A$  domain, with only a slight preference for the middle of the domain. They distribute themselves in a uniform way in the direction parallel to the lamellae. This reproduces the experimental findings of Listak and Bockstaller where, for small tilt grain angles, particles are found to locate somewhat in the center of the preferred domain of the lamellae with no extra aggregation near the tilt boundary; see Fig. 3(a) of Listak and Bockstaller. As the angle is increased, Fig. 2 shows a growing preference of the particles for the kink in the tilt boundary, as shown in panels (b) and (c). This is again consistent with the results of Listak and Bockstaller; see their Fig. 4. This trend continues in Fig. 2(d) where the asymmetric omega grain boundary shows particles with a tendency to aggregate in the central point of the omega shape. Figure 3(b) of Listak and Bockstaller shows this same tendency. Note that the accompanying diagram to their figure actually shows a more symmetric intermediate phase and does not highlight the arrangement of particles away from the omega protrusion which is seen in the micrograph. Figure 2(e) shows a case not studied experimentally, that of the particles preferentially wetting the  $B$  domain. Since the asymmetry found in the omega phase is arbitrary for a symmetric diblock, with either the  $A$  or  $B$  domain forming the omega protrusions, it may be that the addition of nanopar-

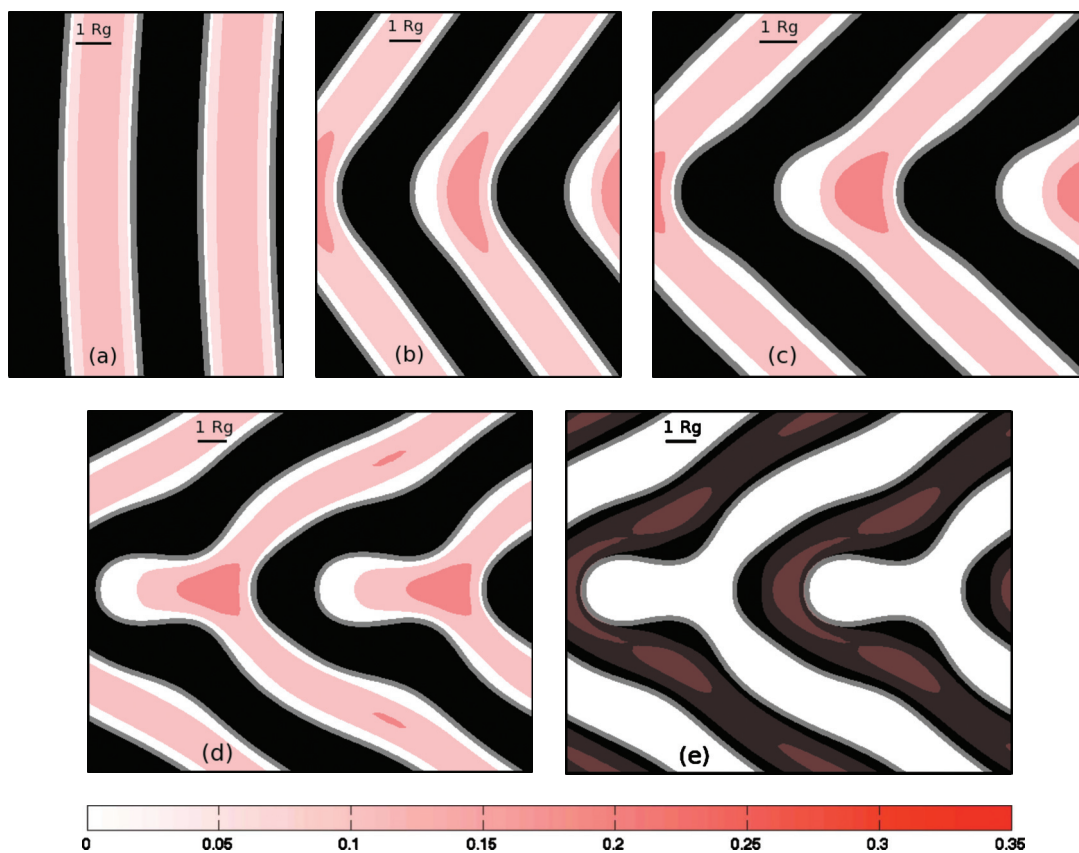


FIG. 2. Tilt grain boundary profiles for a diblock copolymer/nanoparticle composite system. (a) Low angle chevron boundary. (b) Higher angle chevron boundary. (c) Intermediate boundary. (d) Omega boundary. (e) Omega boundary with reversed particle wetting. In all cases except panel (e) the particles are *A* (white contour) wetting. For panel (e) the particles are *B* (black contour) wetting. The gray regions are the *A/B* interfacial regions of *A* from volume fractions of 0.35–0.67. The red indicates regions of higher particle concentrations according to the color bar.

ticles that are preferentially wet by one chemical species will cause the omega protrusion shape to more often form in that chemical species. The free energies of the *A* and *B* preferring particle omega phases are the same within the limit of free energy accuracy of the present calculations. Should it be possible to have particles sequester in the nonprotruding lamella of the omega phase, it is predicted that they will preferentially locate above the omega protrusion and on either side of it, as shown in panel (e).

The particles are seen to prefer those points which correspond to positions of high packing frustration, as indicated by Matsen in his Fig. 4.<sup>6</sup> One exception is that the omega *A* domain shows small regions of slightly higher than background preference on the sides of the omega structure. These secondary points are not shown by Matsen likely because they are, as indicated by Fig. 2, less preferred than the position of highest packing frustration. Listak and Bockstaller hypothesized that particles locate where they do because they relieve packing frustration and allow the polymer to stretch less, just as in the case of added homopolymers.<sup>4,9,10</sup> An advantage of using nanoparticles is that they can be easily distinguished from the polymer and provide a map of regions of high packing frustration. The present theoretical results provide evidence in support of the hypothesis of Listak and Bockstaller, reproducing their regions of highest particle aggregation but also predicting particle locations in

other places they did not observe, locations that are also regions of high packing frustration in diblock copolymer tilt grain boundaries.

One is left to ask why Listak and Bockstaller did not observe particle aggregation in these other regions. Indeed, Fig. 2 shows a much more uniform distribution of particles than observed in experiment. Listak and Bockstaller see either a uniform distribution of particles roughly down the center of the lamellae for low angle chevron boundaries, or complete aggregation of particles in the kink of higher angle chevrons or in the base of the protrusion of omega grain boundaries. One certainty is that the present choice of theoretical parameters does not match their experiments. The SCFT/DFT approach is not expected to be quantitative even if parameters are chosen to try to match experiment, but qualitative trends may be valid. Since the present predictions are observed to be too uniformly distributed, one option is to increase the particle size (in order to reduce the translational entropy of particles for a constant volume fraction) and/or to give the particles a slight preference for themselves over the wetting domain polymer that they are in. This would also more faithfully reproduce the form of “enthalpic neutralization” that Listak and Bockstaller used (see their footnote 7).<sup>11</sup>

Figure 3 shows analogous plots to Fig. 2 but where the  $\alpha$  parameter, which is the ratio of the volume of a particle to the volume of a single diblock molecule, has been increased

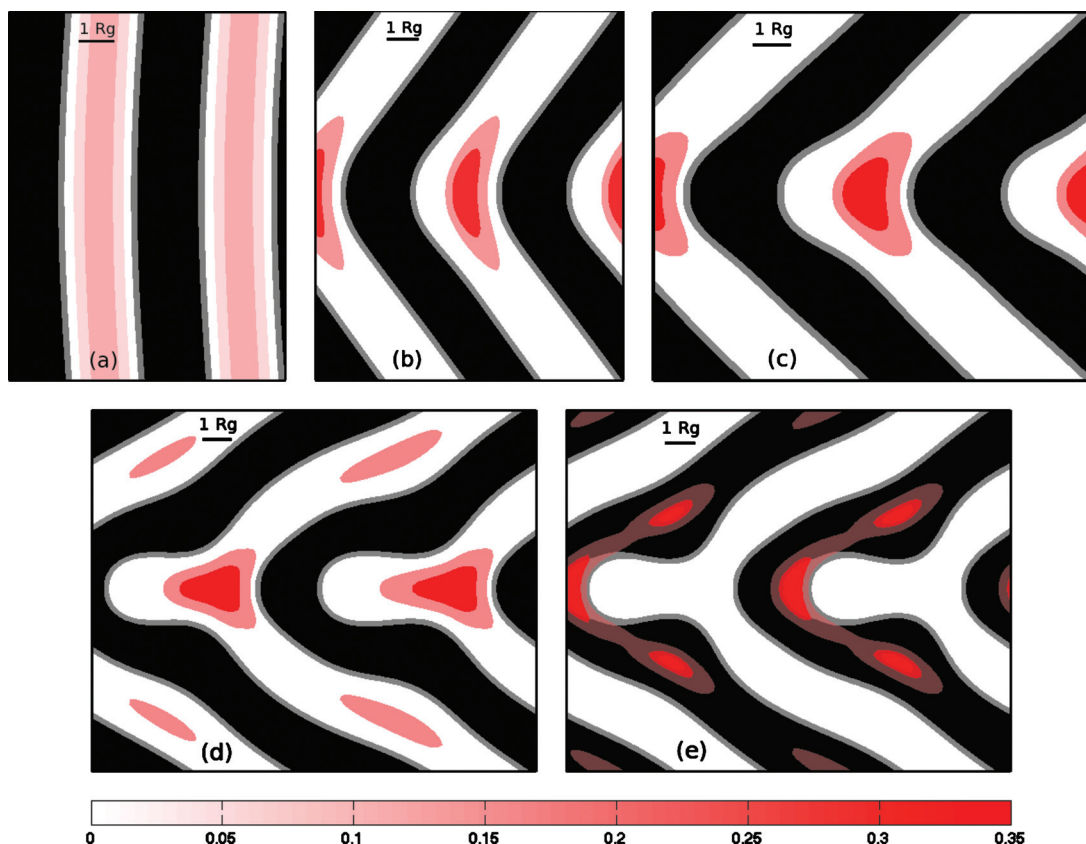


FIG. 3. Same as Fig. 2 but with particles feeling a greater affinity for themselves than for the *A* block [panels (a)–(d)] or *B* block [panel (e)]. The particle volumes have also been increased.

to 2, and the segregation  $\chi_{AP}N$  has been increased to 5. One observes in all panels a greater localization in the particle distributions.<sup>30</sup> In particular, in panel (a), although the particles now prefer the center of the lamellae more, they are still distributed uniformly along the direction parallel to the lamellae. Thus a trend consistent with experiment is found which, if continued, would lead to the strong aggregation of particles in the vicinities of strongest packing frustration while still predicting a more uniform distribution in the center of low angle chevron tilt boundaries. This suggests that if particles could be made more compatible with one block of the copolymer and/or if they could be made smaller, then they could be used to diagnose locations of secondary packing frustration.

#### IV. CONCLUSIONS AND OUTLOOK

It has been shown that the SCFT/DFT hybrid theory is capable of qualitatively reproducing experimental trends for block copolymer nanocomposite tilt grain boundaries. The results provide evidence in support of the hypothesis of Listak and Bockstaller that nanoparticles of appropriate chemistry will gather in regions of high packing frustration of the grain boundaries. The theory predicts that particles interacting more ideally with their wetting block should be able to gather not only in the regions of highest packing frustration but also secondary regions of somewhat lesser packing frustration. Predictions are made for these locations in the no-protrusion domain of the asymmetric omega tilt grain boundary. Further work could involve an increased ac-

curacy examination of particle distributions in the omega phase to see if particles are equally likely to localize in the no-protrusion domain as in the protrusion domain. Trends regarding the frequencies of occurrence of different angles and types of tilt grain boundaries could be calculated. This would be better done in a grand canonical formalism. Other types of grain boundaries could also be examined.

#### ACKNOWLEDGMENTS

The author acknowledges financial support from NSERC.

- <sup>1</sup>M. R. Bockstaller, R. A. Mickiewicz, and E. L. Thomas, *Adv. Mater. (Weinheim, Ger.)* **17**, 1331 (2005).
- <sup>2</sup>C. Park, J. Yoon, and E. L. Thomas, *Polymer* **44**, 6725 (2003).
- <sup>3</sup>C. Park, J. Yoon, and E. L. Thomas, *Polymer* **44**, 7779 (2003).
- <sup>4</sup>M. P. Stoykovich, M. Müller, S. O. Kim, H. H. Solak, E. W. Edwards, J. J. de Pablo, and P. F. Nealey, *Science* **308**, 1442 (2005).
- <sup>5</sup>S. P. Gido and E. L. Thomas, *Macromolecules* **27**, 6137 (1994).
- <sup>6</sup>M. W. Matsen, *J. Chem. Phys.* **107**, 8110 (1997).
- <sup>7</sup>R. R. Netz, D. Andelman, and M. Schick, *Phys. Rev. Lett.* **79**, 1058 (1997).
- <sup>8</sup>Y. Tsori, D. Andelman, and M. Schick, *Phys. Rev. E* **61**, 2848 (2000).
- <sup>9</sup>E. Burgaz and S. P. Gido, *Macromolecules* **33**, 8739 (2000).
- <sup>10</sup>D. Duque, K. Katsov, and M. Schick, *J. Chem. Phys.* **117**, 10315 (2002).
- <sup>11</sup>J. Listak and M. R. Bockstaller, *Macromolecules* **39**, 5820 (2006).
- <sup>12</sup>R. B. Thompson, V. V. Ginzburg, M. W. Matsen, and A. C. Balazs, *Science* **292**, 2469 (2001).
- <sup>13</sup>R. B. Thompson, V. V. Ginzburg, M. W. Matsen, and A. C. Balazs, *Macromolecules* **35**, 1060 (2002).
- <sup>14</sup>A. C. Balazs, *Curr. Opin. Solid State Mater. Sci.* **7**, 27 (2003).
- <sup>15</sup>A. C. Balazs, *Annu. Rev. Phys. Chem.* **58**, 211 (2007).
- <sup>16</sup>C. I. Ren and Y. q. Ma, *Phys. Rev. E* **80**, 011910 (2009).

- <sup>17</sup>M. K. Gaines, S. D. Smith, J. Samseth, M. R. Bockstaller, R. B. Thompson, K. O. Rasmussen, and R. J. Spontak, *Soft Matter* **4**, 1609 (2008).
- <sup>18</sup>L. Zhang, J. Lin, and S. Lin, *Macromolecules* **40**, 5582 (2007).
- <sup>19</sup>R. B. Thompson, K. O. Rasmussen, and T. Lookman, *Nano Lett.* **4**, 2455 (2004).
- <sup>20</sup>J. Y. Lee, A. C. Balazs, R. B. Thompson, and R. M. Hill, *Macromolecules* **37**, 3536 (2004).
- <sup>21</sup>Y.-S. Sun, U.-S. Jeng, K. S. Liang, S.-W. Yeh, and K.-H. Wei, *Polymer* **47**, 1101 (2006).
- <sup>22</sup>J. J. Chiu, B. J. Kim, G.-R. Yi, J. Bang, E. J. Kramer, and D. J. Pine, *Macromolecules* **40**, 3361 (2007).
- <sup>23</sup>M. W. Matsen and R. B. Thompson, *Macromolecules* **41**, 1853 (2008).
- <sup>24</sup>P. Tarazona, *Mol. Phys.* **52**, 81 (1984).
- <sup>25</sup>N. F. Carnahan and K. E. Starling, *J. Chem. Phys.* **51**, 635 (1969).
- <sup>26</sup>M. W. Matsen, in *Soft Matter*, edited by G. Gompper and M. Schick (Wiley-VCH, Weinheim, 2005), Vol. 1, pp. 87–178.
- <sup>27</sup>Packing frustration is the tendency of block copolymer systems to form interfaces of equal thickness, thus preventing undue stretching of polymer molecules and reducing the conformational entropy contribution to the free energy (Ref. 31). This effect is balanced by the tendency to reduce interfacial energies which would, in the absence of packing frustration, promote structures of constant mean curvature (Ref. 32).
- <sup>28</sup>R. B. Thompson, K. Ø. Rasmussen, and T. Lookman, *J. Chem. Phys.* **120**, 31 (2004).
- <sup>29</sup>A lamellar phase is first stabilized within the calculation box, oriented in a diagonal fashion with respect to the box, using periodic boundary conditions. Then, the boundary conditions of two opposite sides of the box are changed from periodic to reflecting and the structure is reconverged. Only the upper (lower) half of the box is needed to show one tilt grain boundary thus formed, although it is repeated (reflected) to best illustrate the entire tilt structure.
- <sup>30</sup>For simplicity, only two contours are shown in Fig. 3. In fact, a nonzero probability of finding particles exists away from the kinks, similar to Fig. 2 but to a much smaller extent. The bulk condition of the lamellae would be that found in Figs. 2 and 3 near the boundaries (away from the kinks). Thus, the systems in these figures, or between panels in each figure, would not correspond to exactly the same overall volume fraction. A comparison between the figures is still appropriate given the qualitative nature of the study in that the trends are still valid. For a quantitative comparison, one should vary the overall particle volume fractions to find equal chemical potentials. A grand canonical formalism would be more convenient for such a study.
- <sup>31</sup>M. W. Matsen and F. S. Bates, *Macromolecules* **29**, 7641 (1996).
- <sup>32</sup>E. L. Thomas, D. M. Anderson, C. S. Henkee, and D. Hoffman, *Nature (London)* **334**, 598 (1988).